Notch Fatigue Life Estimation of Ti-6Al-4V Alloy for Biomedical Implant Applications: A Biomechanical Materials Study

Dr. Michael Johnson[1]*, Dr. Emily Carter[1]

[1]Department of Biomedical Engineering and Orthopedic Materials Science, Mayo Clinic, Rochester, USA

ABSTRACT

It is well known that combination of multiaxial cyclic loading and geometrical discontinuities (such as notches and holes) frequently occurs in engineering practice, and different methods are available in the literature for multiaxial notch fatigue analysis. In such a context, a new analytical approach is here proposed in order to assess the fatigue lifetime of notched components. Such an approach consists in the joint application of (i) the multiaxial high-cycle fatigue criterion by Carpinteri et al. (formulated in terms of stresses on the critical plane) and (ii) the Critical Distance Theory by Taylor (in the form of the Line Method). In order to evaluate the accuracy of the proposed approach, experimental data, recently published in the literature and related to severely notched specimens under uniaxial and multiaxial fatigue loading, are examined, being the specimens made of Ti-6Al-4V, material attracting significant interest by leading industries, such as the biomedical one.

KEYWORDS: critical distance; critical plane; notch; multiaxial; titanium

1. INTRODUCTION

Fatigue failure of engineering components invariably starts from sites of stress concentrations originated by defects and geometrical discontinuities, such as notches, holes, threads, changes in shaft diameter **[1,2]**. In particular, stress concentration phenomena produce localised zone of high stress gradients, resulting in higher driving forces for crack initiation and growth.

Engineers engage in fatigue design of structural components try to minimise the severity of the above geometrical discontinuities by adopting, for instance, large fillet radii and stress relief grooves. However, in practical applications, it is often not possible to avoid sudden changes in components cross section and, consequently, the local stress state at geometrical discontinuities may be over 3-4 times that of the nominal stress.

The effect of geometrical stress concentration on fatigue failure is often studied by analysing specimens weakened by both blunt and sharp notched **[3,4]**. Note that the presence of a notch gives rise not only to stress concentration phenomena, but also to high stress gradients from the notch toward the centre of the specimen. Moreover, even in the case of nominal uniaxial cyclic loading, a multiaxial stress state always occurs close to the notch root. As was suggested by Susmel **[5]**, the implication of this fact is that two types of multiaxiality may take place in an actual engineering component, and more precisely:

(i) *external multiaxiality* related to the applied cyclic loading;

(ii) *inherent multiaxiality* related to the geometrical features of the component itself.

The above classification is valid only when the fatigue problem is formulated in terms of local stresses and not nominal stresses, because in this latter case, the only source of multiaxility is due to the complexity of the applied loading. Note that, for a given local stress state, the corresponding fatigue damage has to be the same independently of the type of multiaxiality source.

The combination of multiaxial cyclic loading and geometrical discontinuities (such as notches and holes) is inevitable in engineering practice: typical examples are engine components, including compressor discs and turbines with complex transmission structures under complex multiaxial loading **[6-9]**. The optimised design of the above discontinuity is of crucial importance in order to avoid catastrophic failure and, consequently, to improve the overall performance and reliability of engineering components **[10]**.

In such a context, different methods were developed for multiaxial notch fatigue analysis (see Ref. **[11]** for an up-to-date review of the state of the art). Among them, some researchers assessed the fatigue life of notched components by directly applying classical multiaxial fatigue criteria, with stress state data extracted from the notch root **[12]**. However, when the influence of high stress gradients on fatigue life is neglected, estimations are generally too conservative **[12]**.

In order to overcome such a drawback, since the beginning of the 2000s, several researchers attempted to implement the so-called

Theory of Critical Distance (TCD) within multiaxial fatigue criteria (as an example, see Refs **[12-17]**). By following a similar strategy, the TCD **[18,19]** and the multiaxial fatigue critical-plane based criterion by Carpinteri et al. **[20]** are combined together in order to assess the fatigue behaviour of severely notched specimens, made of titanium alloy, under multiaxial fatigue. In particular, the stress concentration phenomenon is taken into account by the TCD, whereas, thanks to its features, the Carpinteri et al. criterion allows to correctly estimate the influence of multiaxiality degree given by the stress state near the notch root on fatigue life. Note that, the TCD and the Carpinteri et al. criterion have been recently combined together in order to analyse fretting fatigue problems, providing satisfactory results in terms of both crack paths and fatigue life estimations **[21-23]**.

The present paper is structured as follows. **Section 2** briefly reviews the history of the TCD and the state of the art of the TCD implementation within multiaxial fatigue criteria. The basic concepts of both the Carpinteri et al. criterion and the TCD are outlined in **Section 3**. **Section 4** describes the proposed analytical approach, based on the above criterion and theory, to evaluate the fatigue life of notched components. Then, the effectiveness of fatigue life estimation of the proposed approach is evaluated and discussed in **Section 5** by considering uniaxial and multiaxial fatigue data related to circumferentially V-notched specimens, made of titanium alloy Ti-6Al-4V. Finally, the main conclusions are drawn in **Section 6**.

2. THE THEORY OF CRITICAL DISTANCE: A BRIEF REVIEW

The Theory of Critical Distance (TCD) is the name that has been given by Taylor to a group of theories employed to estimate fatigue strength of structural components weakened by both cracks and notches, by considering the stress field in the vicinity of the stress concentrator **[18,19]**.

The history of the TCD began in Germany at the beginning of the last century with the pioneering work carried out by Neuber, who evaluated systematically the notch effects on fatigue strength of mechanical components **[24,25]**. In particular, the Author suggested estimating the fatigue limit of notched specimens by using a reference stress. Such a stress is obtained by averaging the stress over a line, drawn from the notch root, where the length of the above line was assumed to be a material constant. A few years later, Peterson **[26]** suggested simplifying the Neuber's theory by considering as a reference stress only the stress at a material point, located at a certain distance from the notch root, in order to assess the fatigue limit.

It is important to point out that both Neuber and Peterson encountered some difficulties to employ the methods proposed to address practical problems, and more precisely:

(a) the first difficulty was that to correctly describe the linear-elastic stress field in the vicinity of the stress concentrator in actual mechanical components. In order to overcome such a problem, both Neuber and Peterson combined their methods with simplified

formulas for stress analysis, thus obtaining only approximated results;

(b) the second difficulty was that to accurately define the value of the critical distance for each material. Both Neuber and Peterson determined the critical distance only empirically, by means of a fitting procedure performed on experimental data.

By fully exploiting the theories of Neuber and Peterson, Taylor formalised the theoretical framework of the TCD **[19]**. In particular, according to the TCD, notched components are assumed to be under fatigue limit condition when a suitable effective stress range, $\Delta\sigma_{eff}$, equalled the material plain fatigue limit range. The value of $\Delta\sigma_{eff}$ may be calculated in different ways, and more precisely, after the definition of a suitable critical distance, different integration domains may be adopted. As suggested by Taylor **[19]**, the critical distance, defined as the material characteristic length, L, is calculated as a function of the threshold stress intensity factor range and the fatigue limit range of plain specimens, both measured at the same loading ratio **[27]**. Note that, the value of L for metallic materials can be also evaluated by taking into account a microstructural parameter, namely the material grain size **[19]**.

As mentioned above, by varying the integration domain employed to calculate $\Delta\sigma_{eff}$, the TCD can be formalised in different ways **[19]**, that is:

(a) according to the *Point Method* (PM), $\Delta\sigma_{eff}$ is calculated as the range of the maximum principal stress at a material point located at a distance equal to $L/2$ from the notch root;

(b) according to the *Line Method* (LM), $\Delta\sigma_{eff}$ is calculated by averaging the range of the maximum principal stress along the notch bisector over a distance equal to $2L$;

(c) according to the *Area Method* (AM), $\Delta\sigma_{eff}$ is calculated by averaging the range of the maximum principal stress over a semi-circular area, centred at the notch root, and having a radius equal to L;

(d) according to the *Volume Method* (VM), $\Delta\sigma_{eff}$ is calculated by averaging the range of the maximum principal stress over a hemisphere, centred at the notch root, and having a radius equal to $1.54L$.

It is important to point out that the AM and VM received much lesser attention than PM and LM, because of their more complicated formulations.

As previously mentioned, different approaches, based on the joint application of a multiaxial fatigue criterion and the TCD, were proposed in the literature in order to accurately assess the fatigue strength of notched components. In particular, the approach proposed by Susmel and Taylor deserves to be mentioned **[5,13,28]**. The Authors reformulated the Modified Wöhler Curve Method (MWCM), based on the critical plane approach, in terms of the TCD. Among the TCD formalisations, the MWCM was applied in terms of the PM, due to the

fact that in presence of complex loading it is easier to determine the stress state at a single point rather than to perform average procedures, according to the LM, AM and VM. Thanks to the systematic theoretical and experimental work performed by Susmel and Taylor, it is possible to state that such an approach is highly accurate, since it is able to correctly estimate the high-cycle fatigue strength of notched components, independently of stress raiser sharpness and complexity of the applied loading.

Most of the fatigue criteria implementing the TCD determine the stress state in the surroundings of the notch by taking full advantage of commercial Finite Element (FE) software packages **[29]**. It is important to underline that when FE analyses are performed, generally some model simplifications has to be adopted. In particular, two are the common simplifications **[19]**:

(a) low mesh density: when the mechanical component to be modelled is very large or the features of interest are too small or sharp, the stress field is determined by means of a coarse mesh. Consequently, the obtained results are usually non-conservative and inaccurate;

(b) defeaturing: when some features of the original component are missing or simplified in the analyses, the simplified model gives too-conservative predictions.

Note that, also approximated analytical formulations are available in the literature in order to estimate the stress distribution in notched components **[30]**. Such formulations can be easily implemented in spreadsheets, provide more manageable results

with respect to the sparse data output obtained by means of FE analyses, and make explicit to understand the role played by all the geometrical parameters involved. Without missing the doubtless advantages of FE analyses, analytical formulations available in the literature for V-notch are herein employed to compute the stress state ahead of notches subjected to both Mode I **[31]** and Mode III **[32]** loading.

In conclusion, it is worth noting that the TCD is highly accurate not only when is employed to address the notch fatigue problem but also when it is used in other structural integrity fields, as is reported in detail in the book written by Taylor **[19].**

3. THEORETICAL FRAMEWORK

3.1 The multiaxial fatigue criterion by Carpinteri et al.

Fatigue life of metallic structural components subjected to multiaxial cyclic loading, under high cycle fatigue (HCF) regime, can be assess by exploiting the Carpinteri et al. criterion **[20]**. Such a criterion, formulated in terms of stress, is based on the so-called critical plane approach, and allows for computing the fatigue life at a critical material point (named P_{cr} in the following) by using an equivalent stress amplitude, together with a unique material reference curve, i.e., the S-N curve. According to such a criterion, the procedure to determine the orientation of the critical plane is detailed below.

Let us consider the stress state at point P of a generic structural component and a generic time instant t of the fatigue loading history. The principal stresses σ_1, σ_2 and σ_3 (with $\sigma_1 \geq \sigma_2 \geq \sigma_3$) and the corresponding principal directions 1, 2 and 3 (identified by means of the principal Euler angles ϕ, θ and ψ) can be computed. Since the principal directions are generally time-varying under multiaxial fatigue loading, Carpinteri et al. suggested to compute the averaged principal stress directions $\hat{1}, \hat{2}$ and $\hat{3}$ by averaging the principal Euler angle values **[20]** (**Figure 1**). In particular, the above averaged directions correspond to the instantaneous ones at the time instant for which the maximum principal stress σ_1 attains its peak value within a loading cycle.

Figure 1

Subsequently, the unit vector $\mathbf{w}$, normal to the critical plane, is assumed to be linked to the $\hat{1}$-direction through an off-angle δ (**Figure 1**) computed by the following empirical expression **[20]**:

$$\delta = \frac{3\pi}{8}\left[1 - \left(\frac{\tau_{af,-1}}{\sigma_{af,-1}}\right)^2\right] \quad (1)$$

where $\tau_{af,-1}$ and $\sigma_{af,-1}$ are the material fatigue strength, at a given number of loading cycles, under fully reversed shear stress and under fully reversed normal stress, respectively.

Finally, the multiaxial fatigue limit condition can be written by equating an equivalent uniaxial stress amplitude, $\sigma_{eq,a}$, to the fatigue strength $\sigma_{af,-1}$:

$$\sigma_{eq,a} = \sqrt{N_{eq,a}^2 + \left(\frac{\sigma_{af,-1}}{\tau_{af,-1}}\right)^2 C_a^2} = \sigma_{af,-1} \quad (2)$$

with:

$$N_{eq,a} = N_a + \sigma_{af-1}\left(\frac{N_m}{\sigma_u}\right) \quad (3)$$

where N_a and N_m are the amplitude and mean value of the normal stress component (perpendicular to the critical plane), respectively; C_a is the amplitude of the shear stress component, lying on the critical plane. Moreover, σ_u is the material ultimate tensile strength. Note that, an equivalent normal stress amplitude, $N_{eq,a}$, is introduced in Eq. (2) instead of N_a in order to take into account the detrimental effect of a tensile mean stress (superimposed on an alternating normal stress) on the fatigue strength of metals. Such an equivalent normal stress amplitude is based on the well-known linear relationship between N_a and N_m (see **Eq. (3)**), described by the diagram of Gooodman **[20].**

Moreover, by exploiting the Basquin relationship for both fully reversed normal and shear stresses, the number of loading cycles to failure, $N_{f,cal}$, is obtained from the following equation through an iterative procedure:

$$\sigma_{eq,a} = \sqrt{N_{eq,a}^2 + \left(\frac{\sigma_{af,-1}}{\tau_{af,-1}}\right)^2 \left(\frac{N_{f,cal}}{N_0}\right)^{2k} \left(\frac{N_0^*}{N_{f,cal}}\right)^{2k^*} C_a^2} = \sigma_{af,-1}\left(\frac{N_{f,cal}}{N_0}\right)^k \quad \textbf{(4)}$$

where k and N_0 are, respectively, the inverse slope and the reference number of loading cycles under fully reversed normal stress, and $k*$ and N_0^* are, respectively, the inverse slope and the reference number of loading cycles under fully reversed shear stress.

It is important to highlight that the above stress components (i.e. N_a, N_m and C_a) are defined with respect to the local frame $Puvw$ attached to the critical plane (**Figure 2**), where the u-axis is defined as the intersection between the critical plane and the plane defined by $\mathbf{w}$ and Z-axis (where the v-axis forms a right-handed system together with u- and w-axis).

In order to determine the above stress quantities, let us consider the stress vector $\mathbf{S_w}$, related to the above critical plane orientation. $\mathbf{S_w}$ may be decomposed in two components, that is: the normal stress vector, $\mathbf{N}$, and the shear stress vector, $\mathbf{C}$ (**Figure 2**). More precisely, at a given time instant, t, the stress vector $\mathbf{S_w}$ can be computed through the following expression:

$$\mathbf{S_w} = \boldsymbol{\sigma} \cdot \mathbf{n} \quad \textbf{(5)}$$

being $\boldsymbol{\sigma}$ the stress tensor at point P and $\mathbf{n}$ the unit vector related to the w-axis. Consequently, the vectors $\mathbf{N}$ and $\mathbf{C}$ can be evaluated as:

$$\mathbf{N} = \left(\mathbf{n} \cdot \mathbf{S_w}\right)\mathbf{n} \quad \textbf{(6a)}$$

$$\mathbf{C} = \mathbf{S_W} - \mathbf{N} \quad \text{(6b)}$$

Figure 2

Since $\mathbf{N}$ is a vector with a periodic modulus and a fixed direction, the corresponding amplitude, N_a, and mean value, N_m, in a loading cycle can be easily computed. On the other hand, since $\mathbf{C}$ is a vector with a time-varying direction, the definition of the corresponding amplitude, C_a, is not unique and several methods to evaluate such an amplitude are available in the literature. In this paper, the amplitude C_a is computed by means of the Maximum Rectangular Hull method proposed by Araújo et al. **[33]**. More precisely, such a method considers rectangular hulls bounding the closed shear path Σ (**Figure 3**). Each rectangular hull is characterised by both its two sides and an orientation ξ related to an arbitrary direction fixed with respect to time. The half values of the rectangle sides can be computed as follows:

$$C_{i,a}(\xi) = \frac{1}{2}\left[\max_{0\le t<T} C_i(\xi,t) - \min_{0\le t<T} C_i(\xi,t)\right] \qquad i = 1,2 \quad \text{(7)}$$

and C_a is defined as the shear stress amplitude value which maximises the following expression:

$$C_a(\xi) = \max_{0 \le \xi \le \frac{\pi}{2}} \left[\sqrt{C_{1,a}^2(\xi) + C_{2,a}^2(\xi)} \right] \quad (8)$$

Figure 3

More details about the implementation of the above method within the Carpinteri et al. criterion can be found in Refs **[34,35]**.

3.2 The Line Method by Taylor

The position of the critical material point, P_{cr}, where to perform the fatigue life assessment, is here determined by means of the Taylor TCD in the form of the Line Method (LM) **[18,19]**.

Let us consider a traction-free notch surface contained in a specimen subjected to cyclic loading and a point (named hot-spot, H) on the notch surface (**Figure 4**). Such a point is assumed as the point experiencing the maximum value of the maximum principal stress, σ_1 (see **Figure 4**, where point H is assumed to be coincident with the notch root). By taking full advantage of the LM, a segment with a length equal to twice the material characteristic length, L, is considered. In particular, such a length is computed by means of the following equation:

$$L = \frac{1}{\pi} \left(\frac{\Delta K_{I,th}}{\Delta \sigma_{af}} \right)^2 \quad (9)$$

being $\Delta K_{I,th}$ the threshold value of the stress-intensity factor range and $\Delta\sigma_{af}$ the uniaxial fatigue limit range, both referred to the same loading ratio, generally equal to $R=0$.

Figure 4.

The critical point P_{cr} is, hence, located at the end of such a segment $2L$, starting from point H and with a critical direction, γ_{cr}, determined by applying the procedure explained in detail in the next Section (**Figure 4**).

4. FORMULATION OF THE NOVEL ANALYTICAL APPROACH

A flowchart of the proposed analytical approach for fatigue life assessment of notched components is provided in **Figure 5.**

Figure 5.

Firstly, the required input data to perform the analysis are:

(1) the specimen geometrical sizes: for a hollow cylindrical specimen, such sizes consist in the diameters of both the net, $D_{\min}$, and gross, $D_{\max}$, section (and consequently the notch depth, $d=(D_{\max}-D_{\min})/2$), the notch opening angle, 2α, and the notch root radius, ρ (see **Figure 4**);

(2) the mechanical and fatigue material properties, that is: the elastic modulus, E, the Poisson's coefficient, ν, the ultimate

tensile strength, σ_u, the threshold stress-intensity factor range, $\Delta K_{I,th}$, the fatigue strength under fully reversed normal, $\sigma_{af,-1}$, and shear stress, $\tau_{af,-1}$, and the inverse slopes of the S-N curves under fully reversed normal, k, and shear stress, k^*;

(3) the remote loading condition: under biaxial loading condition, represented by bending and torsion, the ranges of both the normal, $\Delta\sigma$, and shear, $\Delta\tau$, stress applied to the specimen, the phase angle, β, between the normal stress and the shear stress and the loading ratio, R.

Firstly, the hot-spot H on the notch surface is determined by means of the procedure reported in Sub-Section 3.2. According to the LM, segments starting from H and characterised by a length equal to $2L$ and different orientations (i.e. different values of γ, **Figure 4**) are taken into account in order to perform the fatigue life assessment.

After setting a suitable value of the angular increment, $\Delta\gamma$, the proposed approach starts by considering the initial value $\gamma = 0°$. Then, the stress tensor along the segment with an orientation γ is computed by employing a set of closed form expressions available in the literature [**31**,**32**]. For the sake of simplicity, the stress tensor is computed only in some equally spaced points belonging to the above segment.

It is worth noting that the closed form expressions here employed allow to compute the overall stress field in V-shaped notched components subjected to bending [**31**] and torsion [**32**] loading. In

particular, the above analytical solutions, derived by imposing global equilibrium conditions, were formulated by means of complex potential functions and the actual notch shape. Note that, all the characteristic parameters present in the analytical expressions are only functions of the notch geometry, the stress concentration factors and the remote loading conditions. More details about the analytical solutions employed here can be found in Refs [**30-32,36,37**].

Once the stress state is computed in some equally spaced points belonging to the segment with orientation γ, the Carpinteri et al. criterion is applied to such points. In particular, for each point on the considered segment, it is necessary to the compute the amplitude, $N_a(\gamma,r)$, the mean value, $N_m(\gamma,r)$, of the normal stress and the amplitude of the shear stress, $C_a(\gamma,r)$, on the critical plane, being r the radial coordinate shown in **Figure 4**, with $0 \le r \le 2L$.

It is important to highlight that the above stress components are refereed to the critical plane, generally characterised, from one point to another along the same segment, by different orientations especially in the case of high stress gradients.

In order to consider for each material point a stress quantity not depending on the critical plane orientation, the normal t to the segment with orientation γ is assumed as the reference direction. In particular, the components of $N_a(\gamma,r)$ with respect to the reference frame PXYZ are computed as follows:

$$N_{a,x}(\gamma,r) = N_a(\gamma,r)\alpha_x(\gamma,r) \quad \textbf{(10a)}$$

$$N_{a,y}(\gamma,r)=N_a(\gamma,r)\alpha_y(\gamma,r) \quad (10b)$$

$$N_{a,z}(\gamma,r)=N_a(\gamma,r)\alpha_z(\gamma,r) \quad (10c)$$

where $\alpha_x(\gamma,r)$, $\alpha_y(\gamma,r)$ and $\alpha_z(\gamma,r)$ are the direction cosines of the normal $\mathbf{w}$ to the critical plane with respect to PXYZ.

Then, the component of $N_a(\gamma,r)$ along the t-axis is obtained by means of the following equation:

$$N_{a,t}(\gamma,r)=\beta_x(\gamma,r)N_{a,x}(\gamma,r)+\beta_y(\gamma,r)N_{a,y}(\gamma,r)+\beta_z(\gamma,r)N_{a,z}(\gamma,r) \quad (11)$$

where $\beta_x(\gamma,r)$, $\beta_y(\gamma,r)$ and $\beta_z(\gamma,r)$ are the direction cosines of the normal $\mathbf{t}$ with respect to PXYZ.

Subsequently, for a given segment (that is for a given orientation γ), the average value of $N_{a,t}(\gamma,r)$ is obtained as follows:

$$\overline{N_{a,t}}(\gamma)=\frac{1}{2L}\int_0^{2L}N_{a,t}(\gamma,r)\,dr \quad (12)$$

Then, a new orientation of the segment is taken into account by updating the value of the $\gamma-$angle, that is, $\gamma=\gamma+\Delta\gamma$. The above procedure is iteratively repeated for all the segments belonging to the specimen half-space characterised by $0°\le\gamma\le180°$ (**Figure 4**).

The segment orientation that produces the maximum value of $\overline{N_{a,t}}(\gamma)$ is assumed to be the critical one, $\gamma=\gamma_{cr}$:

$$\overline{N_{a,t}}(\gamma_{cr})=\max_{0°\le\gamma\le180°}\left\{\overline{N_{a,t}}(\gamma)\right\} \quad (13)$$

Once the critical orientation is computed, the critical point P_{cr} is assumed to be located at the end of the segment starting from H, with length $2L$ and orientation γ_{cr} (see **Figure 4**).

By considering the values of the stress components acting at point P_{cr} (i.e. $N_a(\gamma_{cr},2L)$, $N_m(\gamma_{cr},2L)$ and $C_a(\gamma_{cr},2L)$), it is possible to determine the fatigue life, $N_{f,cal}$, by solving Eq.(4).

5. EXPERIMENTAL APPLICATION AND DISCUSSION

In the present section, the above analytical approach is applied to some experimental data recently published in the literature **[38-40]**. Such data are related to uniaxial (pure bending and pure torsion) and biaxial (combined bending and torsion) fatigue tests performed on circumferentially V-notched hollow cylinders. The geometrical sizes of the tested specimens are reported in **Table 1**.

Table 1

The material being analysed is a titanium grade 5 alloy (Ti-6Al-4V), whose static and fatigue properties and chemical composition are reported in **Tables 2** and **3**, respectively.

Table 2

Table 3

The experimental tests were performed through of a flexible test bench, by applying to two external forces exerted by hydraulic actuators (for more details see Ref. **[38]**). In particular, each tested specimen was fixed to the bench by means of friction grips

clamped by four bolts. Moreover, one extremity of the specimen was fixed to a vertical support whereas the other one was bolted to a lever arm. Each servo-hydraulic actuator was equipped with 15 kN load cell and driven by a closed-loop digital controller. The two external forces were derived as functions of the desired values of both normal stress amplitude, σ_a, and shear stress amplitude, τ_a, at the specimen net-section. Moreover, the loading ratio, R, was equal to -1 and the frequency was in the range of 2–8 Hz, depending on the applied load level. The biaxial fatigue tests were characterised by a biaxility ratio, τ_a/σ_a, equal to $\sqrt{3}$ and a phase angle β equal to $0°$ or $90°$.

The experimental data, analytically examined in the following, are reported in **Figure 6** in terms of σ_a against the number of loading cycles for pure bending loading and τ_a against the number of loading cycles for pure torsion and combined bending and torsion loading.

Figure 6

According to the procedure presented in Sub-Section 3.2, the hot-spot H coincides with the notch root, independently to the loading conditions being examined. Then, a segment starting from H, with a length and an orientation equal to $2L$ and γ, respectively, is considered.

As previously mentioned, the value of the critical distance, L, is a function of $\Delta K_{I,th}$ and σ_{af}, according to Eq.(9). Since the value

of $\Delta K_{I,th}$ for Ti-6Al-4V was not measured during the experimental campaign being examined **[38-40]**, L is assumed to be linked to the material average grain size. As is reported in Ref. **[41]**, such a grain size varies between 40 and 100 μm for the titanium grade 5 alloy. Therefore, for bending loading, the critical distance L is assumed to be equal to the lower bound of the grain size range (that is, $2L$=80μm) in order to avoid too non-conservative estimations, due to the fact that the stress gradient decreases very quickly by moving away from the notch root. Pure torsion and combined bending and torsion fatigue loadings, instead, are characterised by higher stress gradients (close to the notch root) than those related to pure bending loading. Consequently, by following an argument similar to that followed in Ref. **[5]**, a critical distance larger than the value adopted for bending loading is considered. More precisely, the critical distance L is assumed to be equal to the upper bound of the grain size range and, hence, the length is equal to 200μm.

Subsequently, the orientation γ is made to vary from $0°$ to $180°$ (with an angular increment equal to $\Delta\gamma = 10°$) and the computed value of γ_{cr} is equal to $90°$ for pure bending fatigue loading, whereas $120°$ for both pure torsion and combined bending and torsion fatigue loading. Finally, the analytical approach previously described in Section 3.1 is applied to the above experimental data.

The results in terms of stress components at the critical material point (that is, $N_{eq,a}$ and C_a) and the corresponding theoretical fatigue life are reported in **Table 4** for bending loading (test No.

1-4), torsion loading (test No. 5-8), in-phase (test No. 9-12) and out-of-phase bending-torsion loading (test No. 13-16).

Table 4

In order to verify if such an approach is able to correctly estimate both experimental failure and run out, the fatigue endurance condition, given by Eq.(2), has to be taken into account. Such a condition is illustrated by the C_a against $N_{eq,a}$ diagram, reported in **Figure 7**.

Figure 7

Each $(N_{eq,a}, C_a)$ point represented in this diagram corresponds to a given experimental test, whereas Eq.(2) defines the ellipse with semi-axis equal to $\tau_{af,-1}$ along the vertical axis, and $\sigma_{af,-1}$ along the horizontal axis. According to the Carpinteri at al. criterion, fatigue failure occurs when the $(N_{eq,a}, C_a)$ point lies out of the ellipse, whereas the safe domain is located inside the ellipse.

From **Figure 7**, it can be observed that the criterion estimates failure for all tests, with the exception of the test No.4. Such results are in quite satisfactory agreement with the experimental ones. More precisely, for test No.3 two specimens were tested within the experimental campaign: one showed failure at about $3(10)^5$ loading cycles, whereas the other one showed run out. Due to the fact that

different tests performed at the same stress level are represented, according to the Carpinteri et al. criterion, by only one point in the C_a against $N_{eq,a}$ diagram, for test No.3 the criterion estimates the specimen failure, whereas for test No.4 correctly estimates run out.

As far as finite life fatigue tests are concerned, the number of loading cycles to failure, $N_{f,cal}$, is computed by employing Eq.(4), and reported in the last column of **Table 4**.

The diagram of $N_{f,cal}$ against N_{exp} (**Figure 8**) proves that the application of the present approach returned results mainly falling within scatter band 3x (i.e. $N_{f,cal}/N_{exp}$ equal to 3 and 0.33), independently of loading condition being examined.

Figure 8

6. CONCLUSIONS

A novel analytical approach has been proposed to estimate the fatigue failure of notched specimens. Such an approach is based on the joint application of the multiaxial fatigue criterion proposed in the past by Carpinteri and co-workers and the Theory of Critical Distance (TCD) by Taylor. In particular, among the different formalisations of the TCD, the Line Method (LM) has been here adopted because it is well known that such a method is able to provide more accurate results with respect to other average procedures such as the Area Method and the Volume Method.

The present analytical approach possesses some advantages with respect to other methods available in the literature, since it implements some analytical formulations in order to estimate the stress distribution in notched components. Consequently, no complex finite element models are needed and the analytical stress field formulations, easily implemented in spreadsheets, are only functions of the notch geometry, the stress concentration factors and the remote loading conditions. Due to their reduced complexity, the above formulations turn out to be very useful in practice.

To validate the proposed approach, some experimental data recently published in the literature and related to severely notched specimens under uniaxial and multiaxial fatigue loading have been examined.

By means of the present approach it is possible to achieve a quite good prediction of the fatigue lives for the above experimental tests, confirming the validity of both the Carpinteri et al. criterion and the TCD in presence of complex multiaxial stress state and high stress gradients.

Quite good estimation of the fatigue life of the above experimental tests has been obtained, together with an accurate evaluation of the fatigue endurance condition.

On the basis of such encouraging results, it is possible to conclude that the proposed analytical approach seems to be able to correctly taking into account both the presence of stress concentration phenomena and the damaging effect of stress gradients in predicting the fatigue life of severely notched components. As

future perspectives of the present research work, it is proposed the application of the analytical approach to other notch geometries, loading conditions and, more in general, in presence of any source giving rise to high stress gradients.

Acknowledgements

The work of Sabrina Vantadori is supported by Italian Ministry of University and Research (P.R.I.N. National Grant 2017, Project code 2017HFPKZY; University of Parma Research Unit).

Additionally, the authors would like to acknowledge Professor Filippo Berto, Professor Alberto Campagnolo, Professor Giovanni Meneghetti for providing the experimental data, and Prof. Michele Zappalorto for the documentation kindly provided.

REFERENCES

[1] Y.Murakami, Metal Fatigue, Elsevier Science Ltd, Amsterdam, 2002.

[2] U. Zerbst, M. Madia, C. Klinger, D. Bettge, Y. Murakami, Defects as a root cause of fatigue failure of metallic components. I: basic aspects, Eng. Fail. Anal. 97 (2019) 777-792.

[3] A. Carpinteri, R. Brighenti, S. Vantadori, Influence of the cold-drawing process on fatigue crack growth of a V-notched round bar, Int. J. Fatigue 32 (2010) 1136-1145.

[4] L.M. Viespoli, A. Johanson, A. Alvaro, B. Nyhus, F. Berto, Strain controlled medium cycle fatigue of a notched Pb-Sn-Cd lead alloy, Eng. Fail. Anal. 104 (2019) 96-104.

[5] L. Susmel, Multiaxial Notch Fatigue, Woodhead Publishing, Cambridge, 2009.

[6] D. Liao, S.P. Zhu, J.A.F.O. Correia, A.M.P. De Jesus, R. Calçada, Computational framework for multiaxial fatigue life prediction of compressor discs considering notch effects, Eng. Fract. Mech. 202 (2018) 423-435.

[7] S.P. Zhu, Y. Liu, Q. Liu, Z.Y. Yu, Strain energy gradient-based LCF life prediction of turbine discs using critical distance concept, Int. J. Fatigue 113 (2018) 33-42.

[8] J. Mateus, V. Anes, I. Galvão, L. Reis, Failure mode analysis of a 1.9 turbo diesel engine crankshaft, Eng. Fail. Anal. 101 (2019) 394-406.

[9] S.P. Zhu, S. Xu, M.F. Hao, D. Liao, Q. Wang, Stress-strain calculation and fatigue life assessment of V-shaped notches of turbine disk alloys, Eng. Fail. Anal. 106 (2019) 104187.

[10] H. Bazvandi, E. Poursaeidi, Effect of additional holes on crack propagation and arrest in gas turbine casing, Eng. Fail. Anal. 111 (2020) 104443.

[11] D. Liao, S.P. Zhu, J.A. Correia, A.M. De Jesus, F. Berto, Recent advances on notch effects in metal fatigue: a review, Fatigue Fract. Eng. Mater. Struct. 43 (2020) 637-659.

[12] D. Liao, S.P. Zhu, G. Qian, Multiaxial fatigue analysis of notched components using combined critical plane and critical distance approach, Int. J. Mech. Sci. 160 (2019) 38-50.

[13] L. Susmel, D. Taylor, The modified Wöhler curve method applied along with the theory of critical distances to estimate finite life of notched components subjected to complex multiaxial loading paths, Fatigue Fract. Eng. Mater. Struct. 31 (2008) 1047-1064.

[14] N. Gates, A. Fatemi, Notch deformation and stress gradient effects in multiaxial fatigue, Theor. Appl. Fract. Mech. 84 (2016) 3-25.

[15] M. Benedetti, C. Santus, Mean stress and plasticity effect prediction on notch fatigue and crack growth threshold, combining

the theory of critical distances and multiaxial fatigue criteria, Fatigue Fract. Eng. Mater. Struct. 42 (2019) 1228–1246.

[16] P. Luo, W.X. Yao, P. Li, A notch critical plane approach of multiaxial fatigue life prediction for metallic notched specimens, Fatigue Fract. Eng. Mater. Struct. 42 (2019) 854–70 .

[17] Z. Namiq, L. Susmel, Proportional/nonproportional constant/variable amplitude multiaxial notch fatigue: cyclic plasticity, non-zero mean stresses, and critical distance/plane. Fatigue Fract. Eng. Mater. Struct. 42 (2019) 1849–1873.

[18] D. Taylor, The theory of critical distances: a history and a new definition. Struct. Durab. Health Monit. 2 (2006) 1-10.

[19] D. Taylor, The Theory of Critical Distances: A New Perspective in Fracture Mechanics. Elsevier Science, Oxford, 2007.

[20] S.Vantadori, A. Carpinteri, R. Luciano, C. Ronchei, D. Scorza, A. Zanichelli, Y. Okamoto, S. Saito, T. Itoh, Crack initiation and life estimation for 316 and 430 stainless steel specimens by means of a critical plane approach, Int. J. Fatigue 138 (2020) 105677

[21] S. Vantadori, G. Fortese, C. Ronchei, D. Scorza, A stress gradient approach for fretting fatigue assessment of metallic structural components, Int J Fatigue 101 (2017) 1-8.

[22] A. Carpinteri, S. Vantadori, A. Zanichelli, Lifetime estimation of mechanical assemblies under constant amplitude fretting fatigue loading, Fatigue Fract. Eng. Mater. Struct. 42 (2019) 1927-1936.

[23] J. Vázquez, A. Carpinteri, L. Bohórquez, S. Vantadori, Fretting fatigue investigation on Al 7075-T651 alloy: Experimental, analytical and numerical analysis, Tribol. Int. 135 (2019) 478-487.

[24] H. Neuber, Zur Theorie der technischen Formzahl, Forsch. Ing. Wes. 7 (1936) 271-274.

[25] H. Neuber, Theory of Notch Stresses: Principles for Exact Calculation of Strength with Reference to Structural Form and Material, Springer Verlag, Berlin, 1958.

[26] R.E. Peterson, Notch sensitivity. in: G. Sines, J.L. Waisman (Eds.), Metal Fatigue, McGraw Hill, New York, 1959, pp. 293–306.

[27] M.H. El Haddad, T.H. Topper, K.N. Smith, Fatigue crack propagation of short cracks, J. Eng. Mater. Tech. (ASME Trans) 101 (1979) 42–45.

[28] L. Susmel, The theory of critical distances: a review of its applications in fatigue, Eng. Fract. Mech. 75 (2008) 1706-1724.

[29] S. SongSong, W. MaoSong, W. Hui, Z. Ying, X.X. Mei, Study of component high cycle bending fatigue based on a new critical distance approach, Eng. Fail. Anal. 102 (2019) 395-406.

[30] S. Filippi, P. Lazzarin, R. Tovo, Developments of some explicit formulas useful to describe elastic stress fields ahead of notches in plates, Int. J. Solids Struct. 39.17 (2002) 4543-4565.

[31] B. Atzori, S. Filippi, P. Lazzarin, F. Berto, Stress distributions in notched structural components under pure bending and combined tractionand bending, Fatigue Fract. Eng. Mater. Struct. 28(2005) 13-23.

[32] M. Zappalorto, P. Lazzarin, S. Filippi, Stress field equations for U and blunt V-shaped notches in axisymmetric shafts under torsion, Int. J. Fract. 164 (2010) 253-269.

[33] J.A. Araújo, A.P. Dantas, F.C. Castro, E.N. Mamiya, J.L.A. Ferreria, On the characterization of the critical plane with a simple and fast alternative measure of the shear stress amplitude in multiaxial fatigue, Int. J. Fatigue 33 (2011) 1092–1100.

[34] J.A. Araújo, A. Carpinteri, C. Ronchei, A. Spagnoli, S. Vantadori, An alternative definition of the shear stress amplitude based on the Maximum Rectangular Hull method and application to the C-S (Carpinteri-Spagnoli) criterion, Fatigue Fract. Eng. Mater. Struct. 37 (2014) 764–771.

[35] A. Carpinteri, C. Ronchei, A. Spagnoli, S. Vantadori, On the use of the Prismatic Hull method in a critical plane-based multiaxial fatigue criterion, Int. J. Fatigue 68 (2014) 159–167.

[36] S. Filippi, P. Lazzarin, Distributions of the elastic principal stress due to notches in finite size plated and rounded bars uniaxially loaded, Int. J. Fatigue 26 (2004) 377–391.

[37] M. Zappalorto, P. Lazzarin, J.R. Yates, Elastic stress distributions resulting from hyperbolic and parabolic notches in round shafts under torsion and uniform antiplane shear loadings, Int. J Solids Struct. 45 (2008) 4879–4901

[38] A. Campagnolo, G. Meneghetti, F. Berto, K. Tanaka, Calibration of the potential drop method by means of electric FE analyses and experimental validation for a range of crack shapes, Fatigue Fract. Eng. Mater. Struct. 41 (2018) 2272– 2287

[39] G. Meneghetti, A. Campagnolo, F. Berto, K. Tanaka, Notched Ti-6Al-4V titanium bars under multiaxial fatigue: synthesis of crack initiation life based on the averaged strain energy density, Theor Appl Fract Mech. 96 (2018) 509-533.

[40] A. Campagnolo, J. Bär, G. Meneghetti, Analysis of crack geometry and location in notched bars by means of a three-probe potential drop technique, Int. J. Fatigue 124 (2019) 167-187.

[41] GE Additive, https://www.ge.com/additive/ (accessed 15 July 2020).

NOMENCLATURE

C_a	amplitude of the shear stress component on the critical plane
$D_{\min}$	net section diameter
$D_{\max}$	gross section diameter
d	notch depth
E	elastic modulus
H	hot-spot
k	inverse slope of the S-N curve under fully reversed normal stress
k^*	inverse slope of the S-N curve under fully reversed shear stress
L	material characteristic length
$\mathbf{n}$	unit vector related to the w-axis
N_a	amplitude of the normal stress component perpendicular to the critical plane
$N_{a,t}$	component of N_a along the t-axis
$\overline{N_{a,t}}$	averaged value of $N_{a,t}$ along a segment
$N_{eq,a}$	equivalent normal stress amplitude
N_{exp}	experimental number of loading cycles to failure
$N_{f,cal}$	calculated number of loading cycles to failure
N_m	mean value of the normal stress component to the critical plane
P_{cr}	critical point where to perform the fatigue life assessment
Puvw	local frame attached to the critical plane
PXYZ	reference frame
$\mathrm{P}\hat{1}\hat{2}\hat{3}$	averaged principal stress frame
R	loading ratio
$\mathbf{S_w}$	stress vector related to the critical plane orientation
$\mathbf{t}$	normal vector to the segment with an orientation γ

$\mathbf{w}$	normal vector to the critical plane
2α	notch opening angle
β	phase angle between normal stress and shear stress
γ	orientation of the segment starting from H and with a length equal to $2L$
γ_{cr}	critical plane orientation
δ	off-angle defining the normal to the critical plane
ρ	notch root radius
σ_a	nominal normal stress amplitude related to the net-section
$\sigma_{af,-1}$	material fatigue strength under fully reversed normal stress at N_0 loading cycles
$\sigma_{eq,a}$	equivalent uniaxial stress amplitude
σ_u	material ultimate tensile strength
$\sigma_1,\sigma_2,\sigma_3$	instantaneous principal stresses
τ_a	nominal shear stress amplitude related to the net-section
$\tau_{af,-1}$	material fatigue strength under fully reversed shear stress at N_0^* loading cycles
$\Delta K_{I,th}$	threshold value of stress-intensity factor range
ν	Poisson's coefficient

Acronyms

AM	Area Method
LM	Line Method
PM	Point Method
TCD	Theory of Critical Distance
VM	Volume Method

Submitted to Engineering Failure Analysis

July 2020

NOTCH FATIGUE LIFE ESTIMATION OF Ti-6Al-4V

Camilla Ronchei[a], Sabrina Vantadori[b]

[a] Department of Civil Engineering, University of Calabria, via Pietro Bucci, 87036 Arcavacata di Rende (CS), Italy

[b] Department of Engineering & Architecture, University of Parma, Parco Area delle Scienze 181/A, 43124 Parma, Italy

Corresponding author: sabrina.vantadori@unipr.it

FIGURES AND TABLES

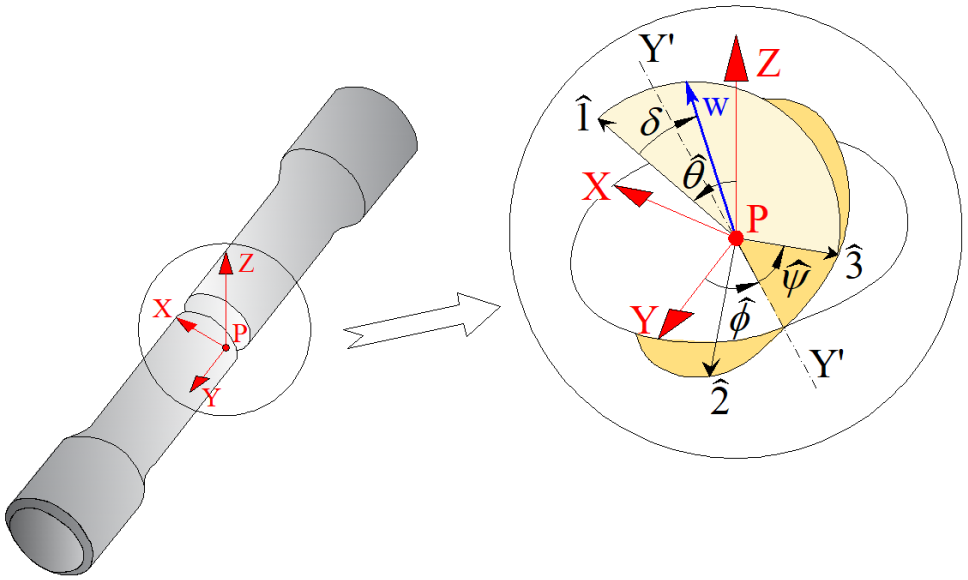

Figure 1. Hollow cylindrical specimen: PXYZ reference frame and $P\hat{1}\hat{2}\hat{3}$ averaged principal stress frame at point P. The normal to the critical plane **w** is also shown.

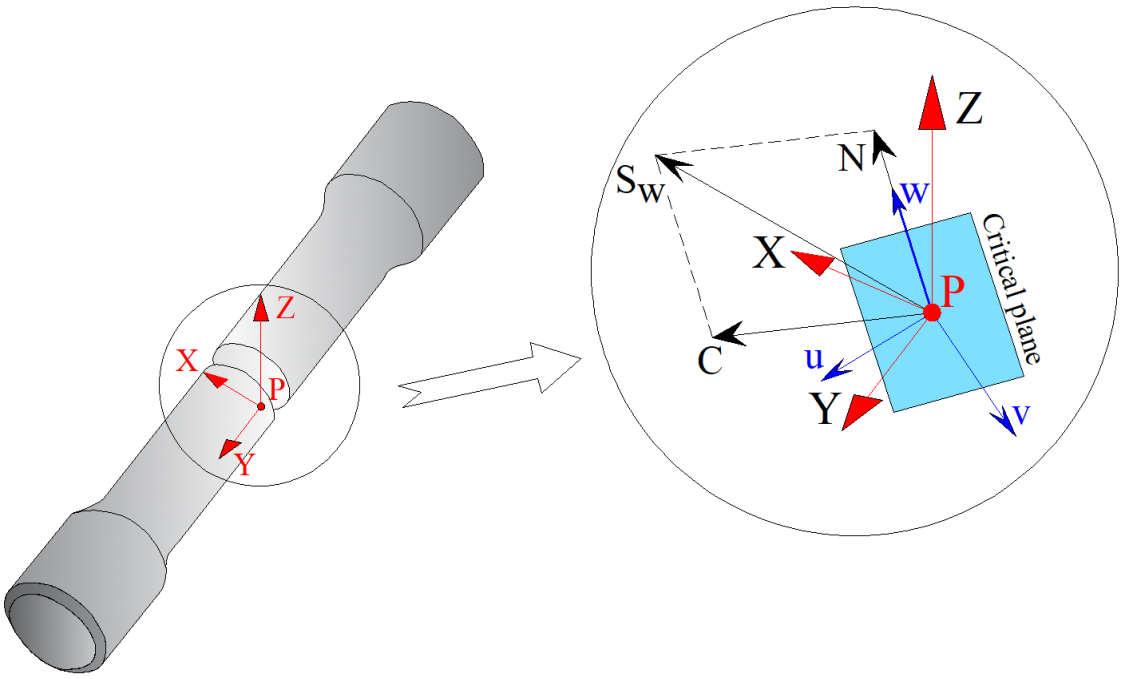

Figure 2. Hollow cylindrical specimen: Puvw local frame at point P and components of the stress vector $\mathbf{S}_w$ acting on the critical plane.

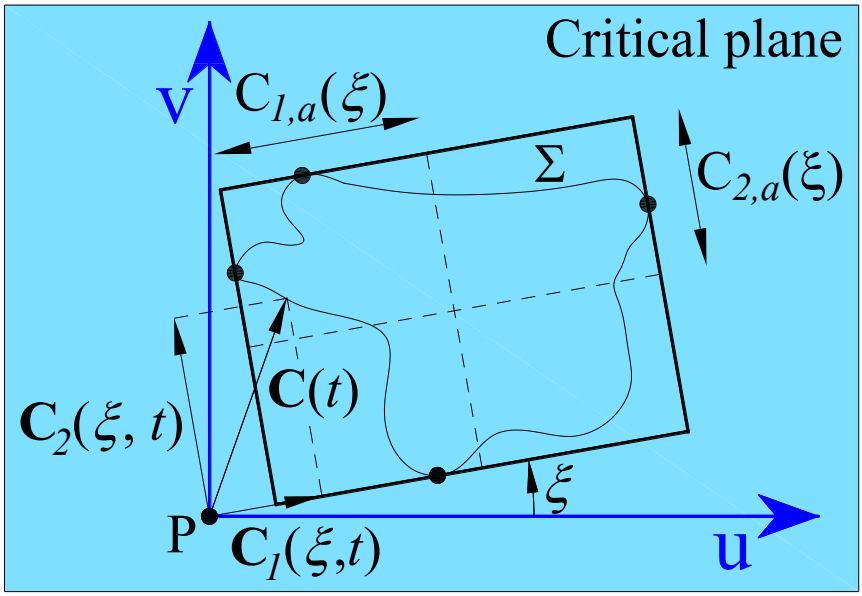

Figure 3. C_a definition according to the Maximum Rectangular Hull method **[33]**.

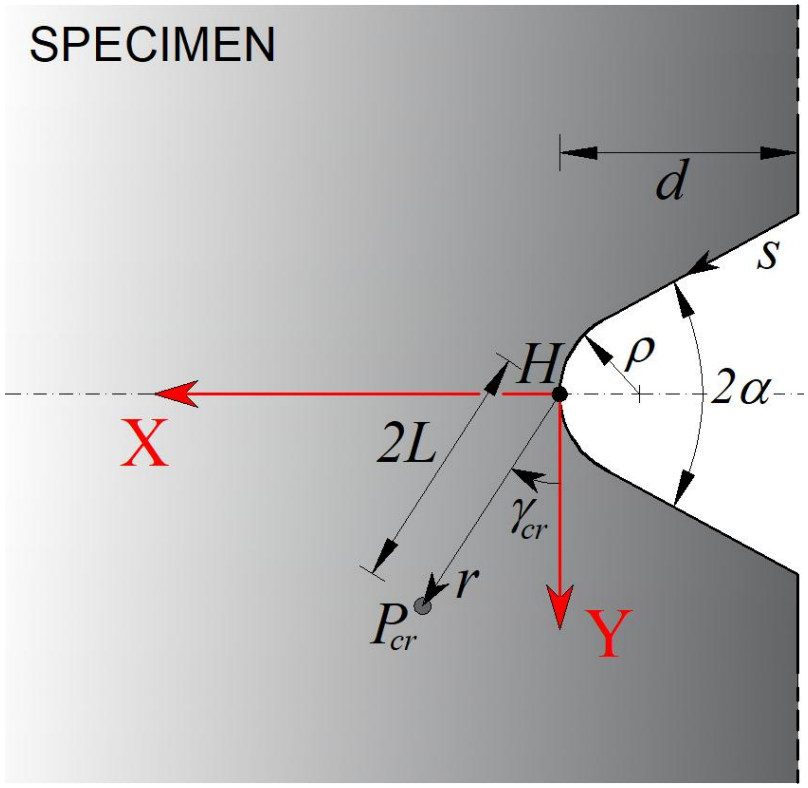

Figure 4. Schematic illustration of the procedure for the determination of the critical material point P_{cr}.

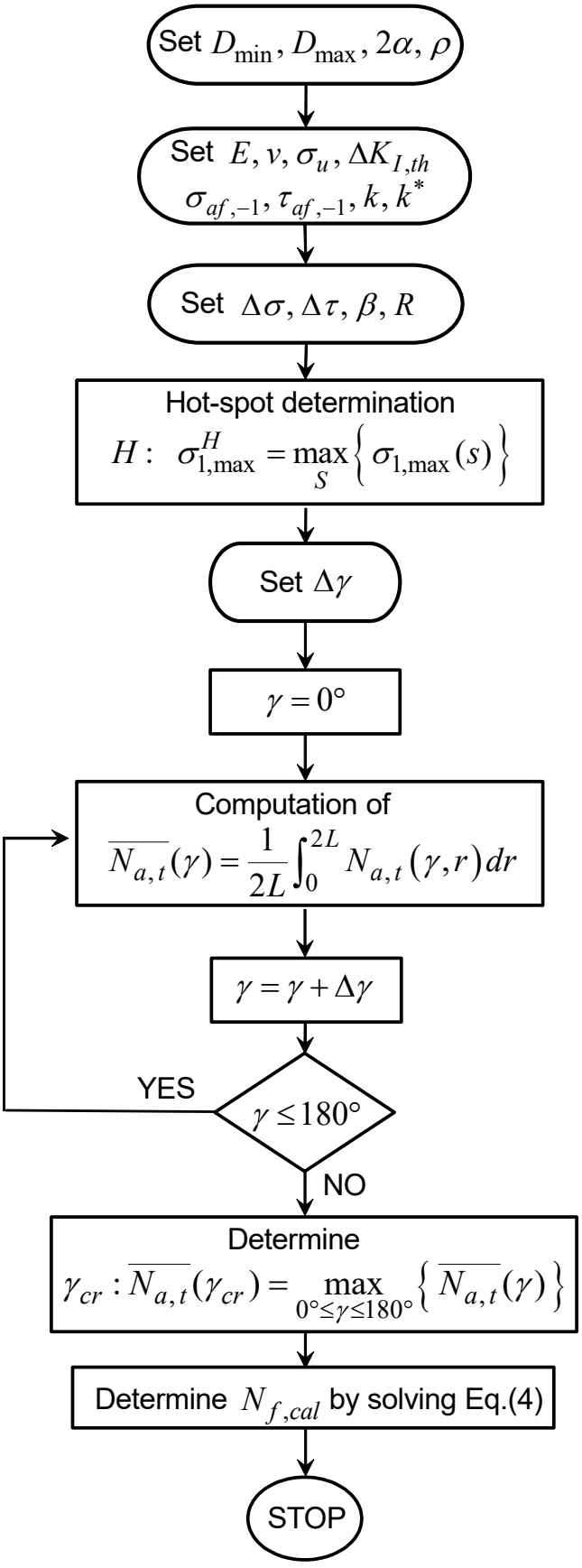
Set $D_{\min}, D_{\max}, 2\alpha, \rho$
Set $E, \nu, \sigma_u, \Delta K_{I,th}$ $\sigma_{af,-1}, \tau_{af,-1}, k, k^*$
Set $\Delta\sigma, \Delta\tau, \beta, R$
Hot-spot determination
$H: \ \sigma_{1,\max}^{H} = \max_{S}\left\{\sigma_{1,\max}(s)\right\}$
Set $\Delta\gamma$
$\gamma = 0°$
Computation of
$\overline{N_{a,t}}(\gamma) = \frac{1}{2L}\int_0^{2L} N_{a,t}(\gamma, r)\,dr$
$\gamma = \gamma + \Delta\gamma$
YES
$\gamma \le 180°$
NO
Determine
$\gamma_{cr} : \overline{N_{a,t}}(\gamma_{cr}) = \max_{0° \le \gamma \le 180°}\left\{\overline{N_{a,t}}(\gamma)\right\}$
Determine $N_{f,cal}$ by solving Eq.(4)
STOP

Figure 5. Flowchart of the novel analytical approach to compute the fatigue life of notched components.

Table 1. Geometrical sizes of the V-notched specimens.

Net section diameter	D_{min}	12 mm
Gross section diameter	D_{max}	24 mm
Notch depth	d	6 mm
Notch opening angle	2α	90°
Notch root radius	ρ	0.1 mm

Table 2. Static and fatigue properties of titanium grade 5 alloy.

E	v	σ_u	$\sigma_{af,-1}$	$\tau_{af,-1}$	k	k^*	N_0	N_0^*
110 GPa	0.3	978 MPa	476 MPa	388 MPa	-0.11	-0.05	$2 \cdot 10^6$	$2 \cdot 10^6$

Table 3. Chemical composition of titanium grade 5 alloy.

Al	V	O	Fe	N	C	H	Residual	Ti
6.05 %	3.98 %	0.15 %	0.13 %	0.003 %	0.02 %	0.001 %	< 0.40 %	Balance %

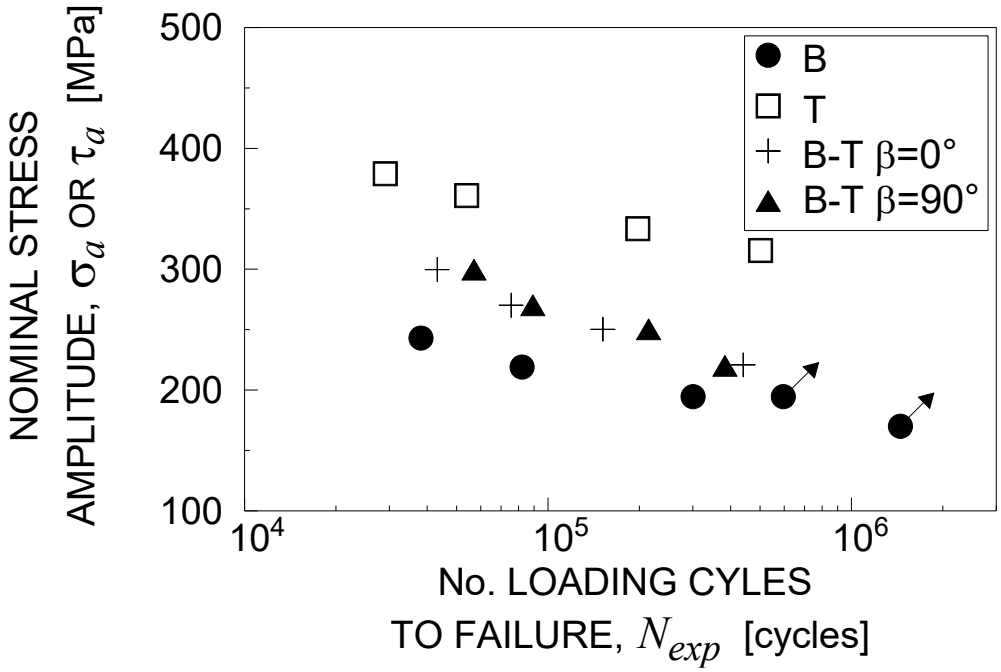

Figure 6. Experimental fatigue data in terms of applied stress amplitude vs No. of loading cycles to failure for: pure bending (B), pure torsion (T) and combined bending and torsion (B-T) loading ($\beta = 0°$ and $\beta = 90°$) **[38-40].** The arrows represent run out conditions.

Table 4. Analytical results in terms of stress quantities on the critical plane and computed fatigue life.

No.	$N_{eq,a}(\gamma_{cr},2L)$ [MPa]	$C_a(\gamma_{cr},2L)$ [MPa]	$N_{f,cal}$ [cycles]
1	621.19	157.15	$9.19\cdot10^4$
2	559.85	141.64	$2.58\cdot10^5$
3	497.21	125.78	$8.30\cdot10^5$
	497.21	125.78	-
4	434.58	109.94	-
5	393.36	394.27	$3.48\cdot10^4$
6	374.68	375.55	$7.48\cdot10^4$
7	346.14	346.94	$2.51\cdot10^5$
8	327.46	328.21	$5.74\cdot10^5$
9	558.95	344.06	$1.67\cdot10^4$
10	549.77	310.18	$3.51\cdot10^4$
11	467.26	287.77	$1.64\cdot10^5$
12	412.25	253.88	$7.56\cdot10^5$
13	417.71	373.77	$4.60\cdot10^4$
14	376.84	336.95	$2.10\cdot10^5$
15	349.40	312.58	$6.12\cdot10^5$
16	334.85	299.50	$1.11\cdot10^6$

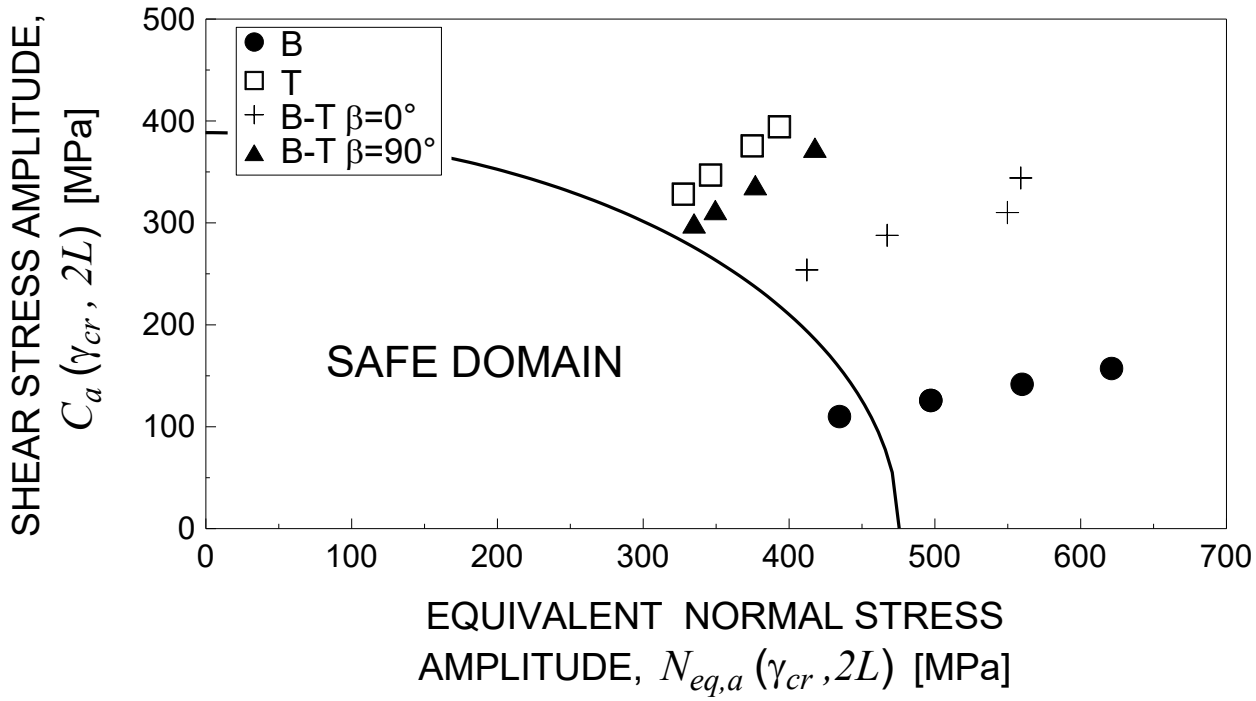

Figure 7. Shear stress amplitude vs equivalent normal stress amplitude: fatigue endurance assessment according to the Carpinteri et al. criterion.

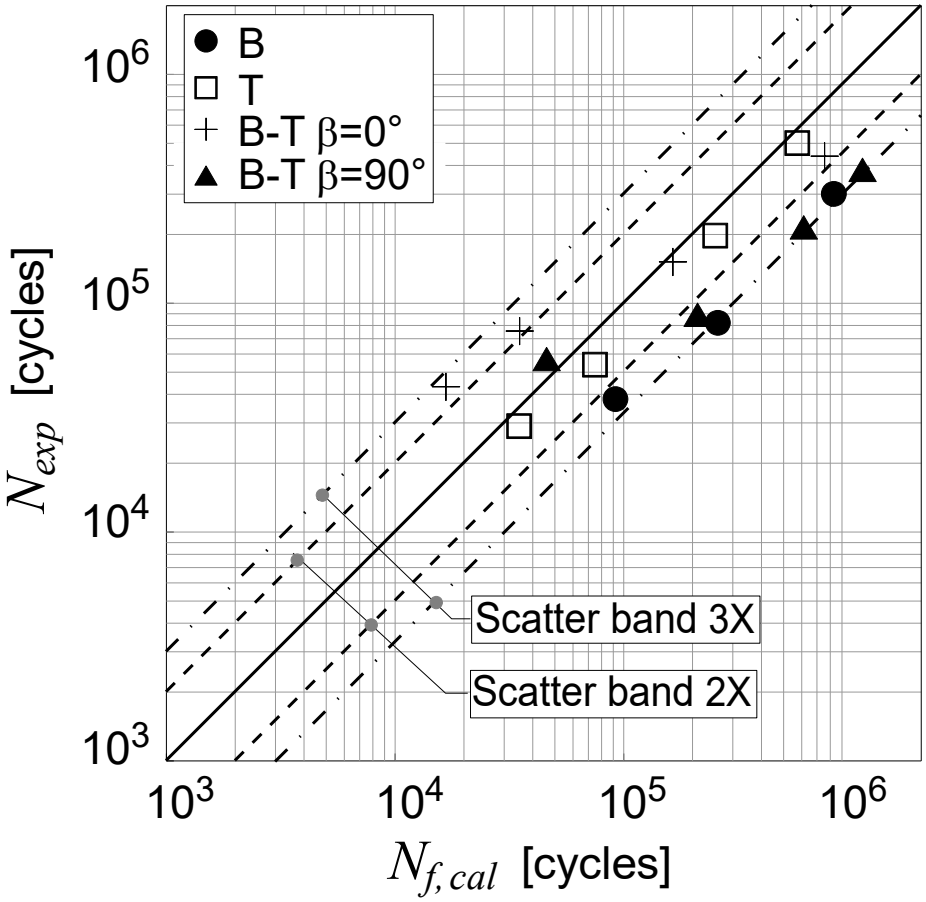

Figure 8. Comparison between analytical and experimental fatigue life.